



# MID-AMERICA TRANSPORTATION CENTER

Report # MATC-MS&T: 129-1

Final Report

WBS: 25-1121-0005-129-1



## 3D Printed FRP-Concrete-Steel Composite Hollow Core Bridge Column

### Chenglin Wu, PhD

Associate Professor  
Zachry Department of Civil and  
Environmental Engineering  
Texas A&M University

### Genda Chen, PhD

Professor and Director of CII  
Department of Civil, Architectural, and  
Environmental Engineering  
Missouri University of Science and  
Technology

### Dimitri Feys, PhD

Department of Civil, Architectural, and  
Environmental Engineering  
Missouri University of Science and  
Technology

### Mohammad ElGawady, PhD

Professor  
Department of Civil, Architectural &  
Environmental Engineering  
Missouri University of Science and  
Technology

### Congjie Wei, PhD

Post-doctoral Associate  
Zachry Department of Civil and Environmental  
Engineering  
Texas A&M University



2024

A Cooperative Research Project sponsored by  
U.S. Department of Transportation- Office of the Assistant  
Secretary for Research and Technology

The contents of this report reflect the views of the authors, who are responsible for the facts and the accuracy of the information presented herein. This document is disseminated in the interest of information exchange. The report is funded, partially or entirely, by a grant from the U.S. Department of Transportation's University Transportation Centers Program. However, the U.S. Government assumes no liability for the contents or use thereof.

MATC

# 3D Printed FRP-Concrete-Steel Composite Hollow Core Bridge Column

Dr. Chenglin Wu  
Associate Professor  
Zachry Department of Civil and  
Environmental Engineering  
Texas A&M University

Dr. Mohammad ElGawady  
Professor  
Civil, Architectural & Environmental  
Engineering  
Missouri University of Science and  
Technology

Dr. Genda Chen  
Professor and Director of CII  
Civil, Architectural, and Environmental  
Engineering  
Missouri University of Science and  
Technology

Dr. Congjie Wei  
Post-doc Associate  
Zachry Department of Civil and  
Environmental Engineering  
Texas A&M University

Dr. Dimitri Feys  
Associate Professor  
Civil, Architectural, and Environmental  
Engineering  
Missouri University of Science and  
Technology

A Report on Research Sponsored by

Mid-America Transportation Center

University of Nebraska–Lincoln

January 2024

## Technical Report Documentation Page

1. Report No. 25-1121-0005-129-1	2. Government Accession No.	3. Recipient's Catalog No.	
4. Title and Subtitle 3D Printed FRP-Concrete-Steel Composite Hollow Core Bridge Column		5. Report Date January 2024	
		6. Performing Organization Code	
7. Author(s) Dr. Chenglin Wu, Dr. Mohammad ElGawady, Dr. Genda Chen, Dr. Dimitri Feys, Dr. Congjie Wei		8. Performing Organization Report No. 25-1121-0005-129-1	
9. Performing Organization Name and Address Missouri University of Science and Technology Rolla, MO 65409  Mid-America Transportation Center Prem S. Paul Research Center at Whittier School 2200 Vine St002E Lincoln, NE 68583-0851		10. Work Unit No. (TRAVIS)	
		11. Contract or Grant No. 69A3551747107	
12. Sponsoring Agency Name and Address Office of the Assistant Secretary for Research and Technology 1200 New Jersey Ave., SE Washington, D.C. 20590		13. Type of Report and Period Covered Final Report Jan 2019 – May 2023	
		14. Sponsoring Agency Code MATC TRB RiP No. 91994-23	
15. Supplementary Notes			
16. Abstract This study aims to investigate a 3D printing method to directly incorporate continuous reinforcement into concrete structures. The ability to design and produce complex structures with optimized topographical configuration can be used to reduce potential material waste while maintaining the required structural strength. Furthermore, the ability to actively incorporate reinforcement into printed members substantially reduces potential labor requirements and eliminates the need to set up formwork. The study began its initial approach with a manual extrusion process containing reinforcement to observe the necessary constraints required to achieve a printing system with this functionality. The second stage of development was designing a preliminary 3D printer with an auger-based extrusion system using a dual-entrance nozzle with the capacity to extrude concrete containing shaped reinforcement. The third phase consisted of controlled testing to simulate the impacts of extrusion rate and setting time on the final bond capacity of cured, printed specimens. A 3D printing platform with a three-axis printing bed was developed with an embedded printing sequence to synchronize the extrusion of concrete and the insertion of the reinforcement. Various combinations of concrete mixes and types of reinforcement were investigated to produce self-sustaining, printed reinforced concrete members.			
17. Key Words		18. Distribution Statement	
19. Security Classif. (of this report) Unclassified	20. Security Classif. (of this page) Unclassified	21. No. of Pages 56	22. Price

## Table of Contents

Abstract.....	vii
Chapter 1 Introduction .....	1
1.1 Overview.....	1
1.2 Research Significance and Objectives .....	3
Chapter 2 3D Printing of Concrete Structures .....	6
2.1 State-of-the-art on Reinforcement Placement in 3D Printing.....	6
2.1.1 Mesh Mould.....	6
2.1.2 Slip Forming .....	7
2.1.3 External Reinforcement Arrangement .....	8
2.1.4 Reinforcement Entraining Device.....	9
2.2 Design Parameters .....	12
Chapter 3 3D Printing Reinforced Concrete Members.....	14
3.1 Manual Extrusion Tests .....	14
3.2 Proposed Automated 3D Printer .....	19
3.2.1 Phase I: Printer Testing.....	21
3.2.2 Phase 2: Reinforcement Printing .....	24
3.2.3 Preliminary Findings.....	25
3.3 3D Printing Reinforcement Members Design.....	26
3.4 Optical Image Analysis.....	30
3.5 Controlled Experimental Testing.....	32
3.5.1 Fresh Preconditioning Pullout Test.....	33
3.5.2 Fresh Bond Pullout Test by Setting Time Variation.....	38
3.5.3 Cured Specimens Rebar Pullout Test .....	39
Chapter 4 Results and Conclusions.....	41
4.1 Results (Phase II) .....	41
4.2 Results (Phase III).....	43
Chapter 5 Conclusions and Recommendations.....	49
5.1 Conclusions.....	49
5.2 Recommendations.....	51
References .....	55

## List of Figures

Figure 2.1 Mesh Mould by ETH Zurich. (Wangler T., Lloret E., et. al, 2016). [3].....	7
Figure 2.2 Smart Dynamic Casting System by ETH Zurich. (Asprone D., Auricchio F., et. al, 2018). [15].....	8
Figure 2.3 External Reinforcement Arrangement. (Asprone D., Auricchio F., Menna C., & Mercuri V, 2018). [15].....	9
Figure 2.4 Reinforcement Entraining Device by TU/e. (Asprone D., Auricchio F., et. al, 2018). [15].....	10
Figure 3.1 Mortar Gun (Manual Configuration).....	16
Figure 3.2 Manual Printing with Flexible “Reinforcement”. .....	17
Figure 3.3 Embedded Wire Reinforcement. ....	18
Figure 3.4 Preliminary 3D Printer Design. ....	20
Figure 3.5 Preliminary Printer. ....	21
Figure 3.6 Unreinforced Printed Truss. ....	22
Figure 3.7 Printing Path. ....	22
Figure 3.8 Printed Non-Reinforced Truss Configurations (a) #1, (b) #2, (c) #3. ....	23
Figure 3.9 3D Printed Truss w/ Steel Mesh (a) before and (b) after. ....	24
Figure 3.10 Final Design for Concrete 3D Printer.....	27
Figure 3.11 Extrusion Nozzle. ....	28
Figure 3.12 3D Printing Process. ....	29
Figure 3.13 Printed Concrete Bars w/ Spiral Reinforcement Extrusion Variation.....	30
Figure 3.14 Fresh Concrete Rebar Pullout Test Setup.....	35
Figure 3.15 Testing Day Preparation Setup.....	36
Figure 3.16 Manual Filling During Pour. ....	37
Figure 3.17 Loaded Specimens for Initial Testing.....	37
Figure 3.18 Landmark Testing Configuration Setup. ....	40
Figure 4.1 Surface Area Defects (a) 150 mm/min and (b) 200 mm/min.....	41
Figure 4.2 Surface Area Voids vs. Reinforcement Area. ....	42
Figure 4.3 Fresh Pullout by Setting Time Variation.....	44
Figure 4.4 Inconsistent Batch Preparations. ....	45
Figure 4.5 Sample Dry Pullout Test Results.....	47
Figure 4.6 Split Concrete Test Sample. ....	48

## List of Tables

Table 3.1 Optical Image Analysis Sample Matrix.....	32
Table 3.2 Preconditioning Pullout Test Matrix.....	36
Table 3.3 Setting Time Test Matrix.....	39
Table 4.1 Fresh Pullout by Setting Time Variation Test Results. ....	45

## Disclaimer

The contents of this report reflect the views of the authors, who are responsible for the facts and the accuracy of the information presented herein. This document is disseminated in the interest of information exchange. The report is funded, partially or entirely, by a grant from the U.S. Department of Transportation's University Transportation Centers Program. However, the U.S. Government assumes no liability for the contents or use thereof.

## Abstract

This study aims to investigate a 3D printing method to directly incorporate continuous reinforcement into concrete structures. The ability to design and produce complex structures with optimized topographical configuration can be used to reduce potential material waste while maintaining the required structural strength. Furthermore, the ability to actively incorporate reinforcement into printed members substantially reduces potential labor requirements and eliminates the need to set up formwork.

The study began its initial approach with a manual extrusion process containing reinforcement to observe the necessary constraints required to achieve a printing system with this functionality. The second stage of development was designing a preliminary 3D printer with an auger-based extrusion system using a dual-entrance nozzle with the capacity to extrude concrete containing shaped reinforcement. The third phase consisted of controlled testing to simulate the impacts of extrusion rate and setting time on the final bond capacity of cured, printed specimens. A 3D printing platform with a three-axis printing bed was developed with an embedded printing sequence to synchronize the extrusion of concrete and the insertion of the reinforcement. Various combinations of concrete mixes and types of reinforcement were investigated to produce self-sustaining, printed reinforced concrete members.

The preliminary results have shown that the quality of printed reinforced specimens decreases as the extrusion speeds increase. The current results do not indicate any significant impacts on bond capacity by varying extrusion rates and setting times.



## Chapter 1 Introduction

### 1.1 Overview

Today's ever-expanding technologies drive the development of new solutions and innovations to tackle existing engineering problems or enable new engineering functionalities. 3D printing is becoming a more coveted means of manufacturing and producing products with a high level of precision along with efficiency. It reduces the amount of physical labor required by having a fully automated system. This type of system significantly reduces the amount of human error and allows for a level of accuracy that is difficult to reproduce consistently in mass. The same is present in the civil engineering field where concrete structures are beginning to be printed with efficiency while maintaining strength and stability [1, 2].

Reinforcement is critical to the strength and performance of concrete structures since the tensile strength of the concrete is almost 10 times less than its compressive strength. Various reinforcing strategies have been incorporated into the 3D printed concrete members. Among them, chopped fiber reinforcement is typically used since it can be easily mixed within the cement paste without affecting the extrusion process significantly. However, this discontinuous reinforcing strategy cannot fulfill the deflection control required, which can only be met by continuous reinforcement. Conventional continuous reinforcement can typically be characterized in several forms. Regarding construction placement, the material can be placed externally or internally to the component that is being reinforced. The material properties can be metallic or even non-metal (A36 steel vs FRP for example). Finally, the material can either be installed passively or prestressed. Conventional construction methods rely on passively installing internal reinforcement which utilize deformed steel bars with a yield strength around 450–500 MPa. This type of reinforcement is inexpensive, ductile, robust and easy to place on site. Reinforcement can

be designed with ribs or indentations to increase the overall bond capacity between the reinforcement and concrete. Additionally, the coefficient of thermal expansion between both concrete and steel is similar, which further amplifies the material's cooperative nature [1,2]. It is imperative to understand that designing a new type/methodology of utilizing reinforcement requires a substantial amount of design, testing, and integration to prove its effectiveness over conventional methods. Since continuous reinforcement provides substantial benefits when incorporated into concrete, it is a necessary element that must be incorporated when considering 3D printing.

The overall benefits of the combination between material and system include: the ability achieve designed strength and ductility, maximized flexibility in terms of free-forming, complex reinforcement configurations, the ability to incorporate sensing technologies such as fiber optic cables, and enabling full automation and geometric optimization. However, there are certain limitations that currently exist and must be researched further before this can be commonly incorporated into practice. These limitations and challenges include: synergic placement of reinforcement in extruded concrete (i.e. the motion and placement of the reinforcement can impact the fresh and cured properties), selecting an ideal reinforcement (the material must have an appropriate surface roughness, stiffness, strength, ductility, and formability), a nozzle design that can accommodate extruding both continuous reinforcement and concrete simultaneously, an intricate computer-aided program to effectively monitor the printing process, and achieving the achieving the desired performance requirements.

Current practices utilizing 3D printing technology for construction still have their own drawbacks that need to be considered during the design process. These challenges include: automated printers are often times ill-equipped to support large scale, complete structures, limited

material types can be used within these machines, the high initial cost and upkeep of the printing technology is often not economical, surface finishes are often low in quality, and the layering of material resulting in potential cold joints [3,4]. These and many other challenges have emerged from the usage of this technology and have not fully been remedied in today's research.

To accommodate these challenges, it is recommended that both computational and experimental investigations on the coupled motion between concrete and reinforcement to determine the underlying rheological impacts, bonding characteristics, and mechanical properties. Furthermore, research should involve selection of material that not only meets the performance requirements but can be easily manipulated while its position remain stationary in the concrete after extrusion.

## 1.2 Research Significance and Objectives

Reinforcement is essential to concrete structures. Not only does it provide the required tensile strength, but also it fulfills the requirement for load bearing capacity, serviceability, and durability. Consequently, the minimum amount of reinforcement needs to be provided to avoid brittle fracturing, ensure ductile behavior by stress redistribution, and control deflections and crack widths. Conventionally, the transverse reinforcement girts or longitudinal members, are positioned in the formwork prior to concrete casting. Which then requires a tremendous amount of installation cost and limited geometrical patterns for the reinforcement. For 3D printing of cementitious materials, the solutions to the reinforcement become even more challenging. As the 3D printing revolutionizes the concrete casting allowing precise control without the need of formwork, the reinforcement becomes an obstacle since it is difficult to be extruded or pumped with the flow of concrete. Most of the current approaches tend to avoid these problems by either using short fiber admixtures to enhance the concrete tensile strength or passively adding

reinforcing mesh layers or steel cables in-between printed layers. These approaches can alleviate the cracking and self-sustaining issues to certain extent, however, are incapable of building realistic large span reinforced concrete (RC) structures that can sustain realistic service loadings.

Typically, pre-installed reinforcement networks or post-installed external reinforcement structures must be utilized to realize the required structural and architectural functions.

Therefore, a direct and tunable reinforcement strategy is needed for 3D printed concrete structures. An integrated configurable reinforcement strategy is proposed, which mechanically forms the reinforcement to desired patterns and geometry within the printed RC structures.

This one-step reinforcement printing strategy will avoid any complications in terms of reinforcement installation and save costs in labor and materials. It also enables the direct printing of RC structures with unlimited reinforcement configuration and arrangement, allowing the architects and engineers to design structures with optimized load-bearing and architectural functions. For instance, a continuously varying spiral reinforcement with a gradual change in pitch distance can be realized to allow precision design of the RC structures subjected to varying external loadings, such as wind load. One can exploit this free-forming concept to input the actual loading distribution from the realistic computational analysis to fully optimize the structural design best suited for the service conditions. The proposed strategy also provides a multifunctional platform for sensing and energy management. For example, wire-shaped, compatible fiber optic sensors can be installed along the configured reinforcement to monitor the temperature and strains during the printing process and under service conditions. Reinforcement with different thermal conductivity and patterns can be integrated to adjust the thermal conductivity of the RC members for energy efficiencies.

To achieve this proposed strategy, the reinforcement has to be allowed to move while being configured mechanically. However, this reinforcement motion introduces several critical issues that need to be addressed such as how to achieve (1) the synergetic placement without shearing the fresh concrete or reinforcement-concrete interface during the printing process, (2) coherent bonding of the reinforcement for the hardened concrete structures, (3) printing sequence and parameters to achieve desired strength for the interlayer, joints, and structures, (4) real-time monitoring of printing quality and structural properties.

However, the current understandings are not sufficient to deal with the above-mentioned issues. Specifically, state-of-art 3D printing analyzes rheology, interfacial bonding, printing monitoring and control which mainly focuses on the interactions between the printed concrete (i.e., moving concrete) with stationary reinforcement. However, the moving reinforcement proposed here request new insights and in-depth understandings on the following topics: (1) the dynamic interaction between the extruded concrete and moving reinforcement, (2) the effects of the moving reinforcement on the microstructures of the concrete at fresh and hardened states, (3) the bond strength at concrete-reinforcement interface, (4) real-time monitoring of the concrete-reinforcement interface during printing process, (5) optimization of printed path and control. Few to nonexperimental or theoretical data are available in these topics, which demands the proposed research in these areas.

## Chapter 2 3D Printing of Concrete Structures

This section presents the literature review of ongoing research in the industry and compares various 3D printing strategies. Various existing approaches will be explained by detailing the overall process in question and reflecting upon the strengths and weaknesses of each system/technique. It should be noted that a detailed rheological discussion is not included within the scope of this project. Finally, there will be a discussion about, specifically, concrete 3D printers utilized in the construction industry today.

### 2.1 State-of-the-art on Reinforcement Placement in 3D Printing

Recent discoveries have revealed the potential to autonomously print concrete along with some form of reinforcement. This reinforcement can be incorporated prior to, during, or after the concrete printing process. Some of the main methods that utilize this technology are the: 1) Mesh Mould, 2) Smart Dynamic Casting System, 3) Reinforcement Entraining Device, and 4) External Reinforcement Arrangement.

#### *2.1.1 Mesh Mould*

The mesh mould method shows that it is possible to develop formwork that also acts as reinforcement. This method was developed at ETH Zurich. This approach utilizes a robotically controlled system to fabricate three-dimensional welded mesh for the reinforcement. The printed mesh is then infilled with special mixed concrete that is able to be locked within the mesh without flowing out. This composite is then encapsulated with the printed thin concrete cover to form the free-form structures. The porous nature of the mesh allows for smooth finishing of concrete to be placed externally outside of the mesh itself. [3,16] This method is seen as beneficial due to the capacity of not only printing complex geometries but allowing the reinforcement to simultaneously act as formwork for the system. However, at its core, it still

requires conventional reinforcement assembly and concrete filling, which limited the structural types and led to multiple-step construction process that has few substantial advantages over conventional construction approach. The system requires each segment to be printed individually before it can be fully assembled into the final structure.

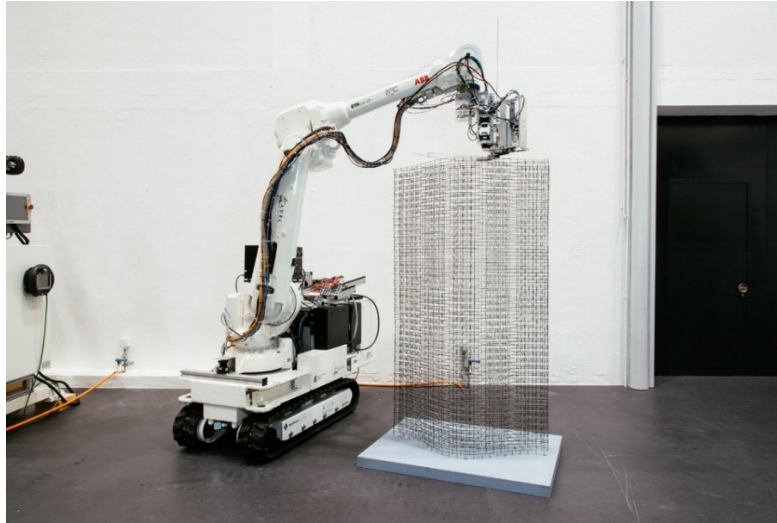


Figure 2.1 Mesh Mould by ETH Zurich. (Wangler T., Lloret E., et. al, 2016). [3].

### *2.1.2 Slip Forming*

Slip forming refers to the process of a material being both continuously poured and formed to the desired geometry. ETH Zurich used this method and developed a system known as Smart Dynamic Casting. This device has moving formwork that is capable of being modified in real time to fit any geometry that is programmed into the device. Furthermore, a built-in sensor monitors the concrete's rheological properties to ensure that the material flows through the formwork and exits the formwork in a hydrated state. This functionality is not typically present in other 3D printers. Rather, a special mix is prepared and used throughout. Being able to effectively monitor and regulate the rheological properties greatly increase the amount of

freedom within a single system. Furthermore, the formwork allows the printed concrete to have a smooth surface and does not require additional finishing like other printers. However, the drawback to the system is that the reinforcement must be altered prior to casting the concrete rather than simultaneously [3, 15, and 16].



Figure 2.2 Smart Dynamic Casting System by ETH Zurich. (Asprone D., Auricchio F., et. al, 2018). [15].

### *2.1.3 External Reinforcement Arrangement*

The external reinforcement arrangement uses sections of 3D printed concrete elements combined with passive reinforcement. Using a truss for example, the concrete is 3D printed into multi-layer extruded segments where a small opening is left at each joint location. A reinforcement frame is then assembled to span the length of the truss with connections inserted into the openings left by the joints. The joints are then filled with concrete mortar similar to how CMU blocks with reinforcement are filled with grout. Once the concrete sections and steel frame



have been connected, the current exterior reinforcement is covered with more layers of 3D printed concrete [15]. One of the main benefits of this system is its ability to topographically optimize the distribution and placement concrete to reduce the amount of material consumption [15] Furthermore, the usage of steel reinforcement provides the designs with the strength and ductility necessary to accommodate for the concrete's weaker properties. However, several issues are still present particularly due to the reinforcement being placed externally as opposed to internally. This can result in the printed design to be more susceptible to environmental degradation, corrosion and interface breakage [16].



Figure 2.3 External Reinforcement Arrangement. (Asprone D., Auricchio F., Menna C., & Mercuri V, 2018). [15].

#### 2.1.4 Reinforcement Entraining Device

The final method explained explores the concept of active reinforcement feeding using flexible steel cable. This device was developed at Eindhoven University of Technology in The Netherlands. The material was chosen both for its ductility and flexibility allowing it to be free forming as it is extruded simultaneously with the concrete. This technique is essentially an advanced version of the Contour Crafting method as passive reinforcement is no longer required.

The mechanism can lay the steel reinforcement in the desired geometric configuration while simultaneously covering the reinforcement in the appropriate amount of concrete [16]. This cable can be embedded in multiple layers of the printed structure.



Figure 2.4 Reinforcement Entraining Device by TU/e. (Asprone D., Auricchio F., et. al, 2018). [15].

A key discovery from this method was that the printed RC beams experienced significantly lower strength and cable slippage (weak interface bonding) than cast concrete. Ultimately, current 3D printing solutions have been shown to be weaker than conventionally cast concrete. Furthermore, conventional, passive methods of incorporating reinforcement are incompatible with the current technologies as they can disrupt the flow path of the concrete and have low bonding strengths. The two main tests performed with this experiment were a pull-out test (cast vs. printed concrete) and a four-point bending test (3 cable types). The specimens were cast as rectangular beams with a cable in the lower section of the beam and printed in layers with

cable at bottom of the beam. Using a displacement-controlled device, the pull-out test was conducted. During the analysis the adhesive bond strength was due to the cable matrix adhesion while the ultimate bond strength was due to a combination of dilatancy, friction, and adhesion. The results of the pull-out test show that the cast concrete's ultimate bond strength is significantly stronger than the printed concrete [17]. This was likely due to significant air voids and imperfections present in the printed matrix as opposed to cast concrete. The printed concrete could not be consolidated like the cast concrete to reduce these imperfections. Furthermore, it was also concluded that the printed concrete had an ultimate bond strength comparable to or less than conventional cast concrete with smooth rebar. The four-point bending test consisted of 3 different cables of varying ultimate stresses and lengths. Each sample was cast into three layers with each layer having a cable. It was concluded that cables with high ultimate stresses failed due to cable slippage, resulting in lower moments than anticipated. While cables with lower ultimate stresses failed at cable breakage with failure moments close to the anticipated values. The resulting factors of this system present the need to further research and find a solution to relative weaknesses of the bond capacity between the printed materials.

The proposed configurable reinforcing concept utilizes a mechanical configuration system to mold the reinforcement into desired patterns and locations. It enables the one-step reinforcement printing process of RC members that are capable of both shear and flexural resistances. However, the moving reinforcement can cause new issues in both the fresh and hardened states. It is currently difficult to quantify or model the effects that continuous, moving reinforcement has on concrete. To solve these problems, the need to advance the current level of scientific understandings in the dynamic concrete-reinforcement interaction, concrete-reinforcement interface bonding, printing process monitoring, and control are necessary to make this technology more applicable.

## 2.2 Design Parameters

3D printing concrete effectively is governed by several parameters that are present in most studies regarding this topic. These concepts include pumpability, extrudability, and buildability. All of these parameters must perform in unison to have a successful print when considering structural components. Pumpability refers to the concrete's ability to be pumped through a system to the nozzle or point of exit. Extrudability refers to the ease the concrete has of being extruded out of a nozzle for printing. This parameter is governed primarily by the concrete's workability. Buildability refers to the concrete's ability to compile multiple layers in each print. This parameter is often governed by the concrete's overall yield strength and workability [20, 21]. Ultimately, the concrete needs to be fluid enough to flow out of the nozzle with ease, yet solid enough to be able to maintain its shape upon extrusion as well as support additional layers of fresh concrete without collapsing [5]. Typically, this requires a balance between admixtures such as accelerators and retarders and a specialized concrete mix. Most researchers seem to keep their actual design mix confidential, however there are some notable similarities between the properties of their mixes. For starters, typically a low w/c ratio (0.25-0.35) is used to provide adequate strength for the concrete once it has been cured. Furthermore, a mix of cementitious materials such as fly ash and silica fume are incorporated further improving the strength and overall workability. Due to the low w/c ratios used, admixtures such as retarders and superplasticizers are required to provide workability and a prolonged settling time to make concrete extrusion more effective [19,22].

There is not a clear, definitive design mix that is perfectly suited for 3D printing applications. However, many designs have been tested and have proven successful. Each specialized mix design, however, considers the three main factors listed above to ensure

adequate and consistent extrusion of the cementitious material. Research regarding environmental impacts to the printed material using these mix designs still needs to be investigated to ensure that the structure can withstand the influences of nature. This information should then be compared to conventional methods environmental strengths further validate benefits from using this technology.

## Chapter 3 3D Printing Reinforced Concrete Members

The following section details the process that led to the development of the 3D Printer utilized in this project. Initial experiments involved manual testing various extrusion methods as well as manually embedding wire into concrete bars to better understand the challenges and limitations that could be found when designing an automated 3D Printer. Upon development of the 3D Printer, reinforced concrete samples were produced by altering the concrete mix, extrusion speeds, and reinforcement configuration. Following these trials, controlled experiments were conducted to simulate the effects of the extrusion process on the bond capacity of the specimens.

### 3.1 Manual Extrusion Tests

This section details the early, manual experiments to determine both a reliable and functional extrusion system method. Furthermore, early incorporation of reinforcement was tested to obtain an observational understanding of the interaction between the reinforcement and concrete. Two main extrusion methods were investigated in this experiment. These included the pressurized extrusion method and the auger-based extrusion method. The pressurized extrusion approach utilizes a piston to directly extrude the concrete mix. However, the gradation in the concrete mix poses serious challenges when applying this approach. A well distributed mix design could not be used for this method due to the limitations of the syringes opening size. The typical opening sizes of the syringe could not accommodate the aggregates particle sizes. Furthermore, initial tests revealed that the syringes capacity was finite relative to other extrusion methods. Essentially, once the piston had extruded the contents of the syringe, the experiment had to be stopped, and the syringe had to be refilled. This substantially reduced the level of

consistency and ability to “print” continuously. These limitations prevented any additional incorporation of reinforcement and therefore were no longer considered as an option.

The most prominent success came with the usage of an auger-based system. An auger extrusion system uses a rotating mechanical “screw” to transport material through a deposition nozzle in a controlled manner. For this experiment a Quikpoint Drill Mate Mortar Gun was used (Figure 3.1). The device was designed to be handheld allowing for easy mobility when conducting manual print tests. The built-in hopper allowed for a larger reservoir of concrete material to be printed continuously. This hopper could be continuously loaded, allowing for larger and longer printed shapes than the syringe. Furthermore, the device came with multiple nozzle attachments allowing the user to have more control over the output shape and aggregate properties. This method was also favored because the user could easily control the extrusion rate with the attached electric drill. In summary the auger-based system was selected for its larger capacity, easy of mobility, custom nozzle configurations, and reliably controllable extrusion rates.

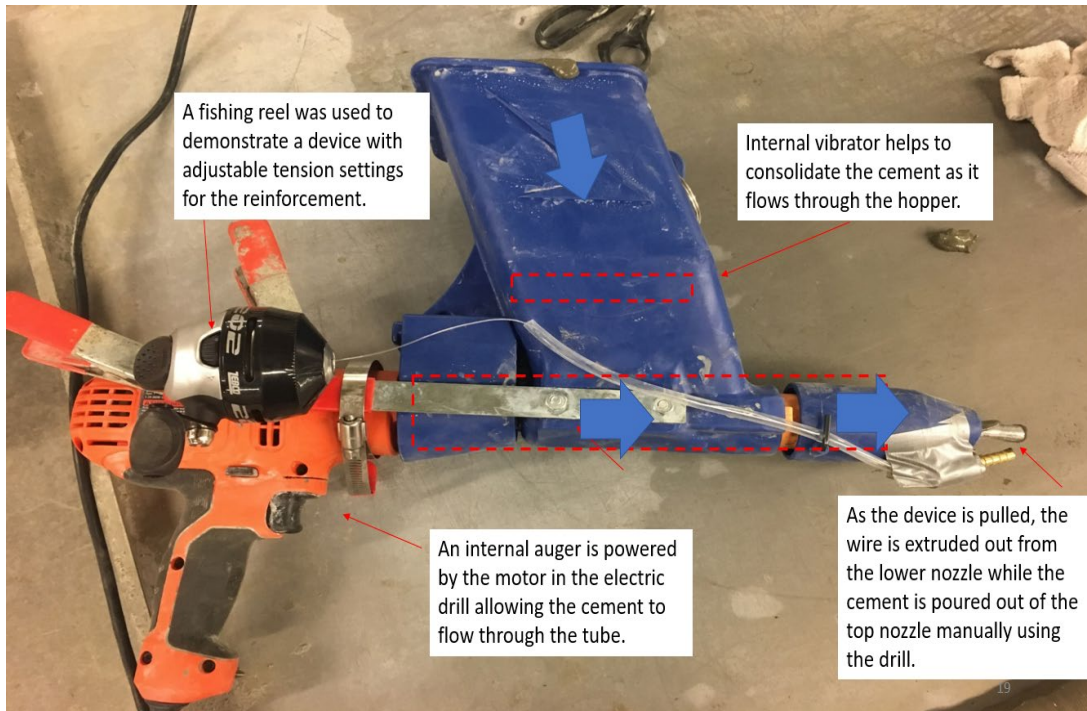


Figure 3.1 Mortar Gun (Manual Configuration).

Initial trials began by extruding mortar with a thin, flexible fishing wire to simulate 3D printing and to get an understanding of the interaction between the two interfaces. The Figure 3.1 below illustrates the mortar gun configuration used for the manual extrusion tests. A fishing reel and wire were used as the “reinforcement” merely to simulate the effects of thin, formable reinforcement. The concept of using flexible “reinforcement” was necessary because 3D printing generally involves complex configurations that deviate from more conventional geometries. Having the capacity to print curved patterns adds a layer of complexity as well as architectural advancement. A fishing reel was selected due to its adjustable tension settings. Tests were conducted using “low” and “high” tension. The goal was to observe the threshold of the concrete’s fresh properties by changing the print direction (i.e. straight line, straight line to a 30° turn, straight line to a 90° turn).



This test would act as a baseline for the design mixes “printing” properties. As for the mix design, several small batches were prepared with varying water to cement (w/c) ratios. Multiple w/c ratios were tested using the mortar gun ranging between 0.25 – 0.50. It was found that higher w/c ratios ( $>0.45$ ) were unable to maintain a self-sustaining shape and were easily impacted by the surrounding environmental vibrations. Lower w/c ratios ( $<0.30$ ) were more than sufficient in maintaining its self-weight however, required significantly more torque to effectively extrude the required amount. Despite the paste being homogeneously mixed, the material would clump together and often clog the exiting nozzle, disrupting the print path. It is also possible that this mix is not fully compatible with the design of the mortar gun. The most consistent success came with a w/c ratio of approximately 0.36. In conjunction with the reinforcement printing experiment, Figure 3.2 below illustrates the print quality of the paste. The material is self-sustaining and requires a low level of torque to print effectively.

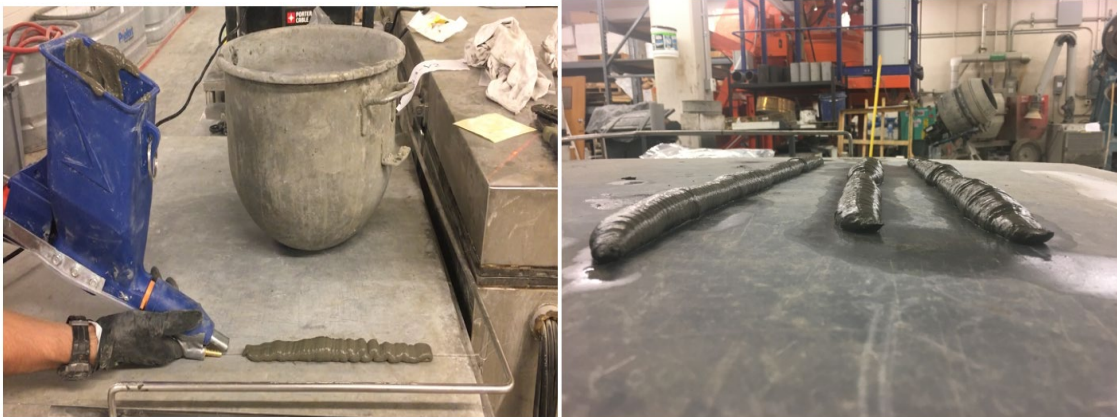


Figure 3.2 Manual Printing with Flexible “Reinforcement”.

Figure 3.2 illustrates the manual attempts of printing concrete along with reinforcement. The fishing reel was selected due to its adjustable tension settings. Manual prints were conducted

using both “low” and “high” tension. Initially, attempts were made to see if, at the lowest tension setting, the friction of the concrete would be sufficient to drag the fishing wire. However, likely due to the low quantity of large aggregates and the general weak state of fresh concrete, the system could not rely on the concrete’s friction alone. The wire itself had to be attached to an exterior surface and would be dragged as the mortar gun was extruding the concrete. As seen, the initial trails proved to be difficult to maintain consistency due to surface vibrations and varying extrusion speeds resulting from a human operator. These inconsistencies can be seen in the lumps or segmental “rings” of the printed specimens. However, it was found that a thin, lightweight material could be embedded throughout the length of the “bar” without disrupting or damaging the shape while simultaneously being supported by the self-weight of the concrete.



Figure 3.3 Embedded Wire Reinforcement.

Figure 3.3 above depicts a wire successfully being embedded into a concrete “bar”. However, due to the wire’s non-adhesive nature, the concrete was not able to effectively bond to the material but rather hardened around the wire with little interface interaction. As such a material with stronger interface bonding capabilities is necessary for reinforcement. The testing also revealed that the material itself was unable to easily conform to different shapes or

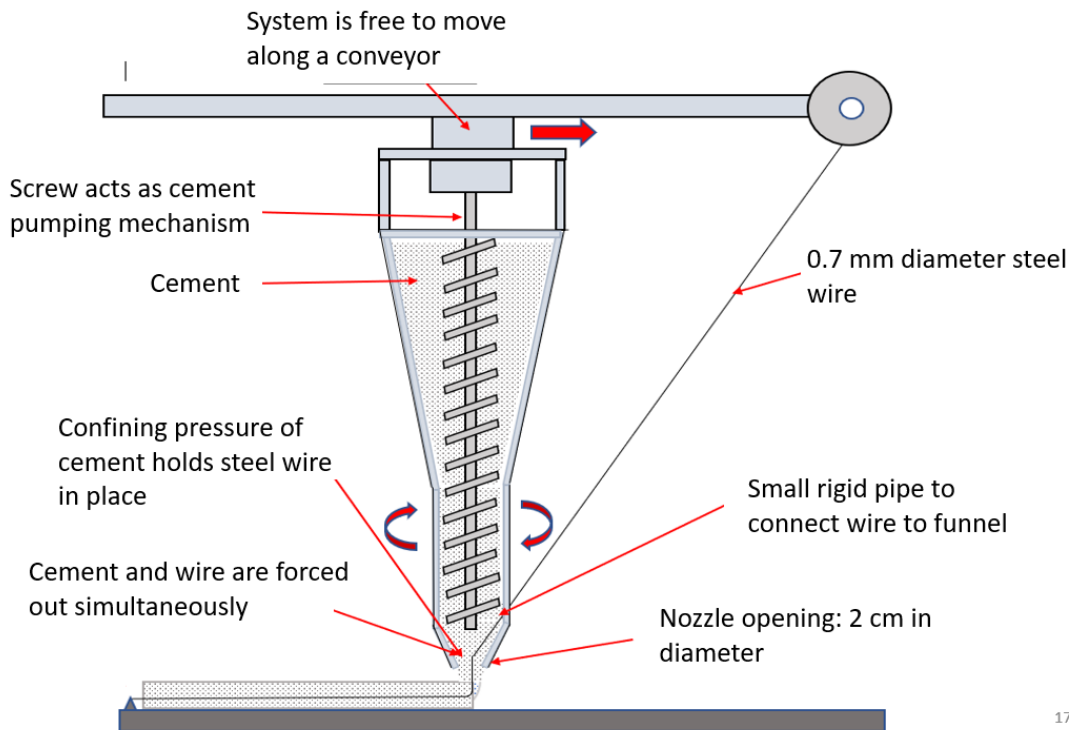
geometries without returning to its original shape due to its semi-rigid properties. As such, making slight or sharp turns while printing caused the fiber to break through the fresh concrete. Even at the lowest tension setting, the required tension to drag the wire out surpassed the strength of the fresh concrete. As such it was concluded that a separate system would need to be designed specifically for the reinforcement to achieve full manipulation of it. Furthermore, a material that is malleable enough to manipulate its overall configuration, yet rigid enough to retain its shape when interacting with the semi-fluid concrete. It was also concluded that the current design mix has limitations in the capacity to withstand alterations to the flow of reinforcement.

### 3.2 Proposed Automated 3D Printer

The next step in the experimental process was to find a method of mounting the auger-based extruder onto a mechanism that could electronically control its movements. Following the design of conventional 3D printers, a gantry system was proposed as a means to accurately control the extruder's movements and flow rate. Figure 3.4 below depicts the early concepts of the proposed 3D printer. The concept was to mount a hanging auger-driven extruder to a gantry system with the reinforcement pinned at one end of the printing surface. The auger would allow consistent, uniform extrusion of the material while having complete control of the quantity extruded. The reinforcement would rely on the self-weight of the concrete and the tension provided by the motion of the gantry on the spooled reinforcement to further drag it along its path as well as to support the reinforcement.

One of the main challenges during this early concept was the ability to move in various directions. Based on the location of the spool, the system could only move linearly in one direction otherwise the tension produced in the reinforcement would damage or break through

the newly printed concrete. As seen later, the final design selected carried this same difficulty throughout the project. This was mainly due to the original configurations' inability to be altered.



17

Figure 3.4 Preliminary 3D Printer Design.

However, due to the reliance on the QuikPoint Drill Mate Mortar Gun, certain changes had to be made to accommodate the premade shape of the mortar gun. Most notably, the mortar gun was supported vertically as opposed to horizontally as seen in Figure 3.5 below. This resulted in the concrete being loaded horizontally due to the mortar gun's hopper configuration. Due to the prefabricated components of the mortar gun initial trials using the new gantry system could not support the addition of reinforcement. Attempts were made by using the fishing wire and feeding it through a small opening (like Figure 3.4). Figure 3.5 below depicts the setup of the

original automated 3D printer with the modified reinforcement attachment. Two tests were conducted under this configuration. The goal was to incorporate reinforcement into the printing process. To accomplish this, initial testing using only the automated extrusion system and paste mix design had to be established. The first test (Phase I) was to test the printer and electrical system's limitations regarding speed, accuracy, and quality of prints. This was accomplished by varying the printer's extrusion speeds, gantry speeds, and printing path designs. By printing samples with the inputs in mind, the system's strengths and weaknesses could be revealed for further improvement. The second test (Phase II) involved incorporating/printing the reinforcement and paste mix as seen in Figure 3.5.



Figure 3.5 Preliminary Printer.

### 3.2.1 Phase I: Printer Testing

Phase I of testing utilized three different truss configurations for design input. The results of these prints can be seen in Figures 3.6 (a,b,c). These truss configurations were selected for

their varying degrees of complexity to test the printer's extrusion quality. The second component major component of this experiment was to match the appropriate gantry movement speed with the extrusion speed. Without harmonious interaction between these two speeds, the final printed specimen would not maintain its required form. Figure 3.6 illustrates the 3D printer designing a simple truss configuration. Figure 3.7 depicts the optimized manually input printing path used to minimize the number of passes during the print cycle.



Figure 3.6 Unreinforced Printed Truss.

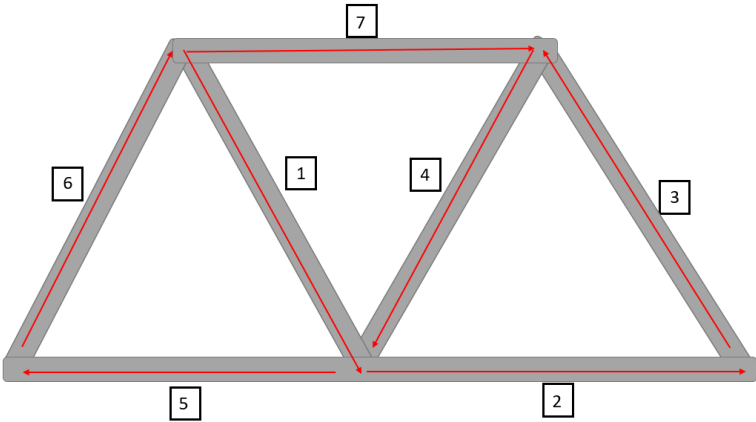


Figure 3.7 Printing Path.

To reach an ideal printing speed vs. extrusion speed with the given extrusion and gantry system, a significant amount of trial and error had to be incorporated to achieve this balance. These tests typically involved printing Truss configuration #1 (Figure 3.8a) until the print quality was visually sufficient. The requirements for this test included: the ability to print the design with no gaps or breaks during the print, uniform printing thickness, and ability to self-sustain at least two printing layers. The final input configuration resulted in a gantry speed to extrusion speed ratio of 1:1 mm/min. This ratio was used for the remainder of the tests. It should be noted that this ratio is not a conclusive idealized ratio for all printers, rather one that worked sufficiently for this project.



Figure 3.8 Printed Non-Reinforced Truss Configurations (a) #1, (b) #2, (c) #3.

Once the printing speeds had become synchronized testing began on printing the three truss configurations seen in the figures above. The printer was successful in printing the required trusses, however there were noticeable defects and issues that would need to be fixed in future projects. All of the printed trusses produced rough, slightly uneven surfaces as opposed to a smooth, consistent surface. This was likely attributed to the high viscosity of the concrete and potential clogging in the nozzle opening. There were multiple instances where the interior of the

nozzle would contain semi-hardened concrete particles that could not extrude properly. The solution to remedy this process was to lightly lubricate the interior of the nozzle and ensure that the material was uniformly mixed so that no large clumps would form. Section 3.3.3 will further address the preliminary findings and limitations of this system.

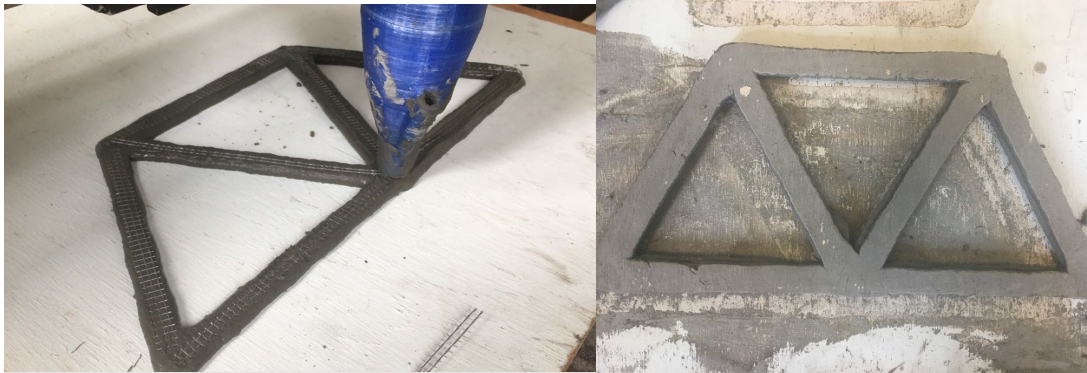


Figure 3.9 3D Printed Truss w/ Steel Mesh (a) before and (b) after.

### *3.2.2 Phase 2: Reinforcement Printing*

Following the initial testing in Phase I, the next goal was to test the paste's ability to support the additional reinforcement and to test the system's capacity to embed reinforcement into the mix. The first test in this phase involved manually laying reinforcement in subsequent layers of the paste to observe how the second layer of paste interacts with the first layer and reinforcement. A fine steel mesh was selected and cut into small strips where it was manually laid on top of a layer of extruded concrete, then covered with another layer of extruded concrete. Figure 3.9a depicts one layer of extruded concrete with the steel mesh overlaid onto the layer. Figure 3.9b depicts the second layer covering the mesh after the concrete has set up. Compared to the previous trials, the finished surface is significantly smoother and more consistent because of ensuring uniform mixing as well as lubricating the nozzle. Furthermore, the embedding of the



steel mesh did not disrupt or damage the surface integrity between layers. Following this test, attempts were made to print a truss using the same concept as seen in Figure 3.4. However, these attempts proved unsuccessful.

### *3.2.3 Preliminary Findings*

A total of four tests were conducted within this portion of the project: 1) testing and determining the appropriate print/gantry speeds, 2) effects on quality by increasing truss configuration complexity, 3) passively (manually) incorporating reinforcement, 4) actively (printing) incorporating reinforcement. It should be noted that the findings within this study are solely based on the capacity of the utilized 3D printer. Upgrading the hardware and overall mechanical system can increase the overall quality and precision in future projects. It should also be noted that the testing conducted through these experiments involved printing objects and different configurations solely. There were not any strength tests performed on the prints. The goals of these experiments were to propose a design concept. Future research will be required to test the overall strength and capacity of these printed specimens.

It was concluded that optimization of print speed and gantry speed are necessary requirements when designing a printer. Without the synchronized interaction between these two parameters, a successful print will not occur properly. Changing the complexity of the design configurations does not impact the mechanical component's ability to perform, however it can potentially disrupt the quality of the printed specimens. Using this system, it was found that a more complex design not only increases lead times but has more potential for error buildup. It was observed that the nozzle would collide material that had already been printed, typically at the truss's "joints". Furthermore, the printer would not fully cover the joint locations, leaving small openings between the printed segments. These issues could potentially be avoided in the

future by optimizing the path configuration for each truss in the future. Optimizing the path configurations would reduce the number of passes the device is required to run to complete the design. Furthermore, this method could ensure that the joints between each leg and segment are properly covered with material to eliminate gaps.

It was found that passively laying reinforcement did not disturb the paste and that multiple layers could bond together with the reinforcement in between. The quality of the layers still requires perfecting, as the reinforcement could be seen sticking out of the printed layers at the corners of the interface. This could be remedied by slightly increasing the extrusion rate of the paste to allow more material to properly disperse over the reinforcement. When attempting to actively extrude reinforcement, it was found that the current configuration is not compatible for this method. The weight of the concrete along with the downward force produced from the extrusion system was not sufficient to overcome the tension produced from the wire being dragged out from a pinned end. Due to this limitation, the system was redesigned to further incorporate active reinforcement feeding. The new system proposed would no longer rely on tension to act as the driving force, but rather a motor would feed the wire through an opening. The following section details the upgraded, final version of the reinforcement entraining concept printer.

### 3.3 3D Printing Reinforcement Members Design

The goal of the project was to 3D print concrete and reinforcement simultaneously. To take it a step further, the added feature of manipulating the geometry of the reinforcement while it was being printed was considered as well. Since 3D printers are coveted for their ability to extrude in various configurations and geometries, adding another degree of freedom in a secondary material (steel reinforcement) further expands the concrete 3D printer's uses.

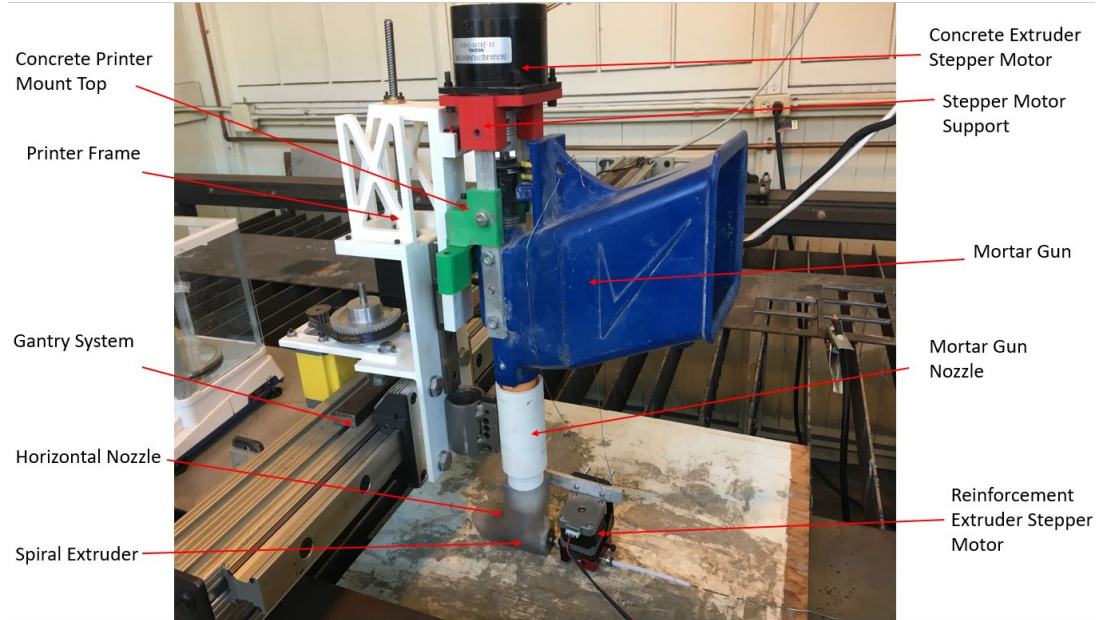


Figure 3.10 Final Design for Concrete 3D Printer.

Figure 3.10 above illustrates the culmination of the various testing and design parameters considered for this thesis. The finalized 3D printer had to be adjusted to actively extrude steel reinforcement simultaneously with the concrete mix. A new custom nozzle had to be designed to accommodate the incorporation of both concrete and reinforcement. Figure 3.11 below shows a detailed view of the conjunction of the two mechanisms.

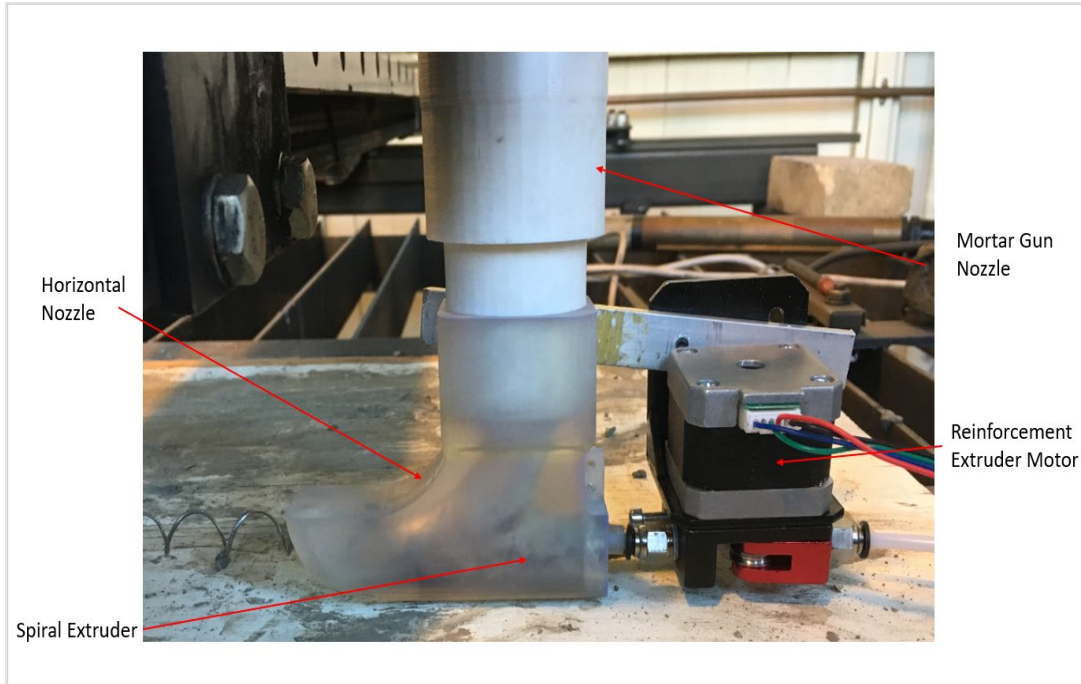


Figure 3.11 Extrusion Nozzle.

The new system is comprised of four major components: the auger-based concrete extruder, the stepper motor powered reinforcement extruder, the reinforcement shaping mold, and the dual-functionality nozzle that produces the concrete and reinforcement. Figure 3.12 below illustrates the process of how each mechanism works. The concrete is extruded through the mortar gun by a stepper motor attached to the top of the device, which allows the auger to rotate and extrude the concrete into the dual-functionality nozzle. Simultaneously, a stepper motor drives two small motor pinions which clasp onto the thin, flexible steel wire and forces it through the reinforcement shaping mold to achieve the desired reinforcement configuration. Once the reinforcement exits the reinforcement shaping mold, it begins interacting with the concrete in the dual-functionality nozzle. This process is driven by two stepper motors which are controlled by manually inputting the desired extrusion speed.

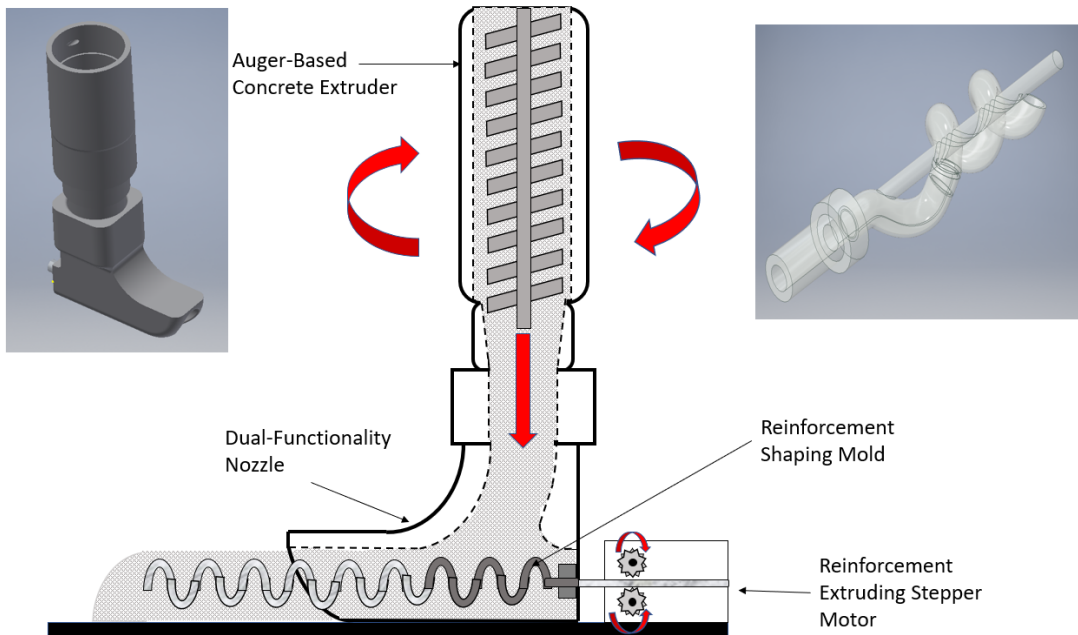


Figure 3.12 3D Printing Process.

A significant amount of trial and error was required to determine compatible speed variations between the two materials. It was found that if the extrusion speeds between the two materials were not synchronized, the quality of the printed bars would be greatly reduced due to the large number of defects and voids within the interface zone. It was observed that at higher reinforcement extrusion speeds, the helix shaped reinforcement would act as an auger, causing the concrete to spread out and away from the reinforcement as it exits the nozzle. As seen in Figure 3.13a below, the results of high reinforcement extrusion speeds and unsynchronized extrusion rates between the two materials show as larger number of defects and openings where the concrete was pushed away by the rotation of the reinforcement. As the rates were slowed and synchronized Figure 3.12c the reinforced concrete bars became more uniform with fewer defects

and voids in the printed specimens. Multiple specimens were then prepared to further be analyzed using an optical microscope (See Section 3.5 for details).



Figure 3.13 Printed Concrete Bars w/ Spiral Reinforcement Extrusion Variation.

Due to the early development stages of this system, there was not a way to accurately monitor the extrusion speeds with various sensors. Rather they had to be inspected visually and recorded for each success and failure. Future work with a stronger electrical/programming system will need to be incorporated before this type of analysis can be properly monitored and analyzed in real time.

### 3.4 Optical Image Analysis

Once the printing process had been established and stabilized, the next goal was to analyze the interface interaction between variations samples using different synchronized extrusion speeds. The quality of large-scale designs cannot normally be viewed at a micro-interface level due to the sheer mass of the completed project. By viewing these small, printed specimens under a microscope, the overall defects and voids within the printing process can be

seen and quantified. It should be noted that for these tests, there were not any failure strength or bond strength tests performed due to the limited number of printed specimens. The objective was to visually see the defects present because of the printing process.

For this experiment, a total of ten specimens were printed at different, yet synchronized extrusion speeds using the helix shaped reinforcement from the process listed in Section 3.4. Table 3.1 illustrates the design matrix for this test. It should be noted that the gantry speed is listed to represent the movement speed of the system (i.e. concrete, gantry, and reinforcement). The concrete and reinforcement extruders have their own separate extrusion speeds; however based on the trials collected, there was not a consistent correlation between the ratios with the given system (i.e. 1:1:2 and 1:2:3 for example). 5 specimens with a w/c ratio of 0.36 (no aggregate) and 5 specimens with a w/c ratio of 0.36 and a sand to binder ratio of 0.75 were printed. The specimens were then cured for 28 days. The specimens were then removed and cut transversely down the center of each bar and a 5 mm long, cylindrical section was cut off and polished to smooth the surface. The samples were then viewed under an optical microscope where the surface area/volumetric defects were analyzed and compared.

Table 3.1 Optical Image Analysis Sample Matrix.

Specimen ID	Gantry movement Speed (mm/min)	w/c ratio	Sand-to-binder ratio
S1503600	150	0.36	N/A
S1603600	160	0.36	N/A
S1753600	175	0.36	N/A
S1903600	190	0.36	N/A
S2003600	200	0.36	N/A
S1503675	150	0.36	0.75
S1603675	160	0.36	0.75
S1753675	175	0.36	0.75
S1903675	190	0.36	0.75
S2003675	200	0.36	0.75

### 3.5 Controlled Experimental Testing

Due to the experimental 3D Printer’s early stages of development, it is currently not possible to effectively monitor and analyze the interaction between the reinforcement and concrete as it is being printed. Therefore, a series of experiments was conducted to simulate the effects observed from the printer. This was achieved by observing the local disturbance and bonding characteristics produced from the displacement/introduction of steel reinforcement within a concrete specimen. One of the main issues initially observed was negative impacts resulting from unsynchronized extrusion speeds. An experiment was conducted to help explain how unsynchronized extrusion speeds can impact the final bond capacity properties. Initially,



one main experiment was to be conducted to simulate these effects. Upon the initial results of the first experiment, a second type was conducted to further support the findings. The first experiment involved performing a “fresh” preconditioning pullout test with varying extrusion speeds. These specimens were then stored for curing. The specimens were then tested using a rebar pullout test after curing for 28 days to determine if the preconditioning effects significantly impacted the final capacity as seen visually from the 3D Printer. The second test involved a fresh pullout test with varying settling times to observe the variations in yield stress and critical strain.

### *3.5.1 Fresh Preconditioning Pullout Test*

The fresh bond capacity test focused on two parameters: disturbance length and displacement rate. The disturbance length refers to the local displacement of the reinforcement relative to the displacement of the concrete. Ideally, the reinforcement and concrete extrusion rate would be equal. Therefore, the resulting relative displacement as viewed locally between the reinforcement and concrete would be equal to zero. This would prevent the concrete from shearing due to the disturbance of the rebar and potentially help with the bond capacity. Due to the early stages of this printer, it cannot be monitored with sensing technology. Therefore, these controlled parameters had to be simulated as a means to further explain the requirement for complete extrusion synchronization.

The second parameter observed was the displacement rate. One major component that was heavily enforced was the idea that the reinforcement and the concrete must be extruded simultaneously at the exact same rate. By using different rates, we can simulate the effects of the reinforcement extruding “faster” relative to the displacement of the concrete and see if there are any adverse effects on the final bond capacity. This way there would be potentially a way to quantify the margin of error allowable for extrusion variation between the two materials. Of

course, the accumulated error over a long span could be substantial. However, the overarching goal in this case was to observe if there are any significant negative effects on the material properties themselves.

The mixed design involved using a w/c ratio of 0.36 and a sand/binder ratio of 0.75. 18” long, 3/8” diameter, ASD 36 mild-rolled, smooth rebar was used as the reinforcement for the experiment. Standard 8” x 4” cylinders will be used for this test. A 3/4” diameter hole will be drilled into the bottom of each cylinder and a 0.5” diameter, 4” long PVC pipe will be inserted through the hole and bonded/sealed with epoxy to prevent any leaking. The inside of the PVC pipe will be lubricated with Vaseline to help reduce friction from the reinforcement and help seal off any leaking into the pipe. A wooden “cap” with a 4” PVC pipe will be inserted through a 3/4” diameter hole in the “cap” and secured with multiple wrappings of Teflon tape around the PVC pipe will be placed over the opening of the cylinder to help center the reinforcement. The PVC pipe was positioned in such a way that only 1.5” of free space between the top and bottom PVC pipes remained. The reinforcement was wrapped in Teflon Tape approximately 3” inches from the base of the bar to a diameter slightly less than that of the PVC pipe. This was to help ensure that no water leaked out of the system. Each batch of concrete was designed for one full set of tests (all three disturbance lengths). First the rebar was placed and held in the center of the cylinder and then covered with the “cap”. Then the concrete was poured into the cylinder up to the full height. The specimens were then consolidated with a consolidation rod. The surface was then smoothed by rolling a consolidating rod while filling any remaining holes with concrete to ensure full consolidation. The specimens were then loaded into the Instron Materials Testing machine and attached to a clamp (Figure 3.14) The tests were run at the varying displacement rates up to the designated disturbance length as seen in Table 3.2. Once the samples had been

displaced to the required length, the samples were “clamped” at the section between the rebar and the cap. This was to prevent the rebar from falling back to its original position once removed from the Instron Materials Testing Machine. The samples were then taken to a cure room and allowed to begin curing for 24 hours before being removed from the cylinder molds. After the specimens had been demolded, they were placed into the curing room for 28 days. Once the specimens had been cured, the final bond capacity test could be completed.

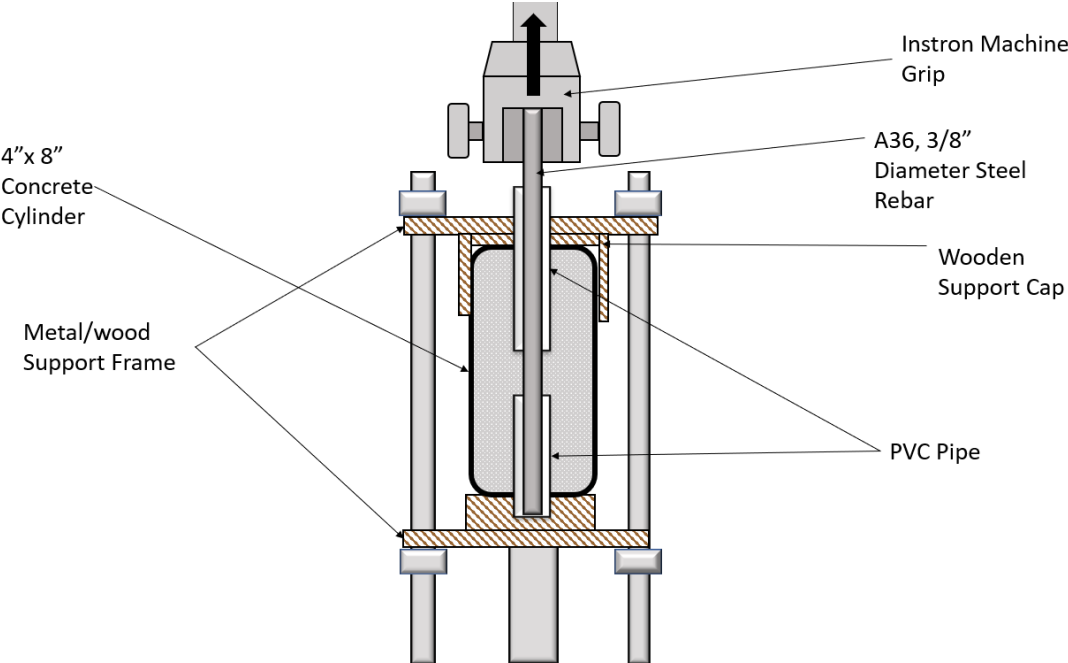


Figure 3.14 Fresh Concrete Rebar Pullout Test Setup.

Table 3.2 Preconditioning Pullout Test Matrix.

Specimen ID	Disturbance Length (inches)	Displacement Rate (mm/min)	w/c Ratio	Sand/Binder Ratio
DD1R5S(1,2,3)	1	0.5	0.36	0.75
DD1R10S(1,2,3)	1	1.0	0.36	0.75
DD1R15S(1,2,3)	1	1.5	0.36	0.75
DD3R5S(1,2,3)	3	0.5	0.36	0.75
DD3R10S(1,2,3)	3	1.0	0.36	0.75
DD3R15S(1,2,3)	3	1.5	0.36	0.75
DD5R5S(1,2,3)	5	0.5	0.36	0.75
DD5R10S(1,2,3)	5	1.0	0.36	0.75
DD5R15S(1,2,3)	5	1.5	0.36	0.75

Figures 3.15, 3.16, and 3.17 illustrate the original concrete pour setup, work performed during the mixing process, and the final result of the loaded specimens.



Figure 3.15 Testing Day Preparation Setup.



Figure 3.16 Manual Filling During Pour.



Figure 3.17 Loaded Specimens for Initial Testing.

### *3.5.2 Fresh Bond Pullout Test by Setting Time Variation*

One of the major challenges with 3D Printing concrete is the impact of settling time on the concrete's overall workability and bond capacity. This is especially true in the case of layered extrusion where cold joints can potentially form. Cold joints are a result of improper bonding between two layers of material. In this case the concrete layers are unable to properly intermix, forming the essential connections at each layer interface. This can result in cracking and early failure due to shear or tension than normally expected. Since this is a common issue for bonding the same material, it is likely that embedding reinforcement into concrete will have a similar problem when it comes to bonding. As soon as cement interacts with water, the chemical bonding process immediately begins and strengthens over time with proper moisture exposure. During the early stages of this project's development, it was observed that there was a relatively short window of opportunity to extrude the concrete without it clogging the nozzle. Therefore, a fine balance between preparation and workability had to be established through trial and error. To further explain the effects that were present in the project, an experiment was conducted to simulate embedding rebar into concrete at various settling times. The goal was to see if the initial bonding capacity is affected by settling time on rebar embedment, like how cold joints are formed between layers.

The mixed design involved using a w/c ratio of 0.36 and a sand/binder ratio of 0.75. 18" long, 3/8" diameter, ASD 36 mild-rolled, smooth rebar was used as the reinforcement for the experiment. Standard 8" x 4" cylinders were cut to 1.5"x 4" to replicate the development length used in the Fresh Pullout Preconditioning test. The cylinders were cut to this size to reduce the quantity of material that had to be produced for each test. This experiment was designed for the

rebar to be completely pulled out of the concrete while in the fresh state. Since the concrete would only be tested in the fresh state, the material used was reduced.

First the rebar was placed and secured in the center of the cylinder with a wooden “cap”. Then the concrete was poured into the cylinder up to the full height. The surface was then smoothed by rolling a consolidating rod while filling any remaining holes with concrete to ensure full consolidation. The specimens were then loaded into the Instron Materials Testing machine and attached to a clamp. The tests were run at a displacement rate of 0.5 mm/min to a displacement of 10 mm. The test matrix can be seen below in Table 3.2. Each concrete mix was tested at 30-minute intervals to note the variation in early bond capacity of the embedded rebar.

Table 3.3 Setting Time Test Matrix.

Specimen ID	Setting Time (min)	w/c ratio	Sand/Binder
WT30B2S(1,2,3)	30	0.36	0.75
WT60B2S(1,2,3)	60	0.36	0.75
WT90B2S(1,2,3)	90	0.36	0.75
WT120B2S(1,2,3)	120	0.36	0.75

### 3.5.3 Cured Specimens Rebar Pullout Test

Once the specimens prepared in the Fresh Preconditioning Test had properly cured, they were tested using the ASTM C900 method for rebar pullout. The samples were tested using an MTS Landmark. The specimens were inserted into a constructed steel frame and had an opening in the bottom surface for the rebar to pultrude outwards. Figure 3.18 below illustrates the configuration of the testing apparatus. A steel plate allowed with shimming material was used to

provide a level surface for the specimens. A neoprene pad was placed under the steel plates and shimming material to be used for compression to prevent any damage to the frame. The steel frame was clamped to the upper grips on the Landmark while the rebar was clamped to the bottom gripper. The samples had an LVDT sensor to measure the relative displacement between the concrete cylinder and rebar. The samples were loaded at 1 mm/minute displacement rate for 10 minutes. The force displacement curves were collected, and the samples were then removed and cut longitudinally to reveal the failure surface plane.

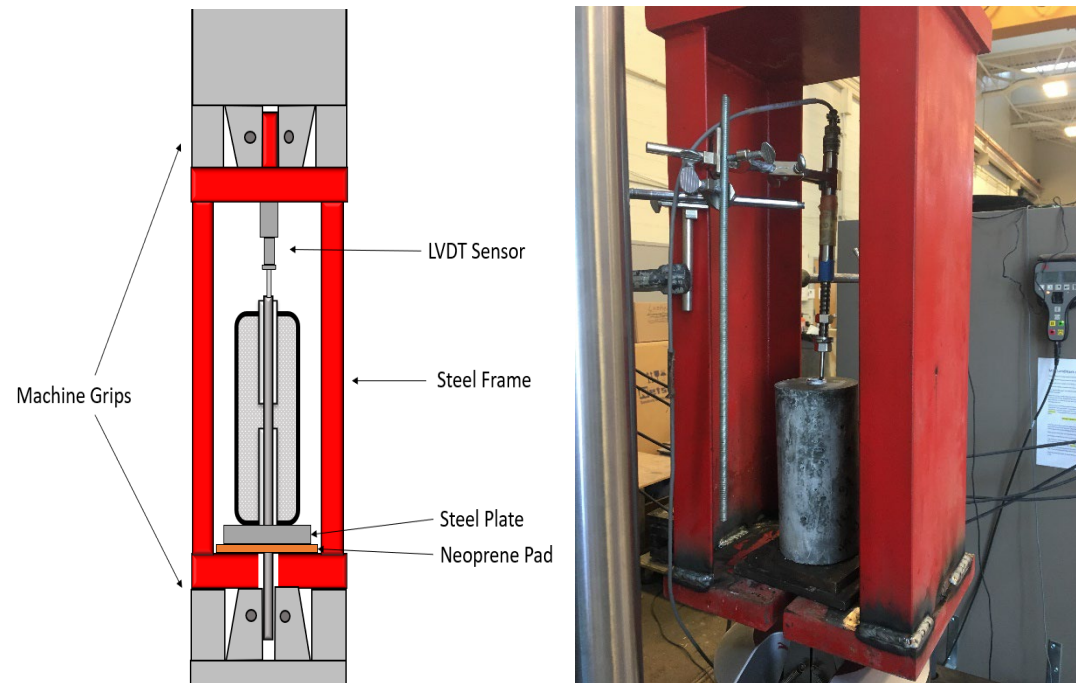


Figure 3.18 Landmark Testing Configuration Setup.



## Chapter 4 Results and Conclusions

### 4.1 Results (Phase II)

The following section details the results brought about by the 3D printing method along with the controlled testing data. During the 3D printing phase, optical images of the printed specimens were taken and analyzed. Using the image analysis system, it was found that the printing speed has an impact on the quantity of surface and volumetric bond defects present. Due to the limitations of the printer itself, print speeds were much slower than that of typical printers. The range of print speeds tested were from 150 - 200 mm/min. Figures 4.1a and 4.1b below show the variation of surface defects brought upon by changing the synchronized extrusion speed rates. Both images below represent samples that did not contain any aggregate. The surface area of the defects was mapped and calculated using an image processing tool. It should be noted that the resolution of the microscope could not accurately determine the volumetric variations in voids.

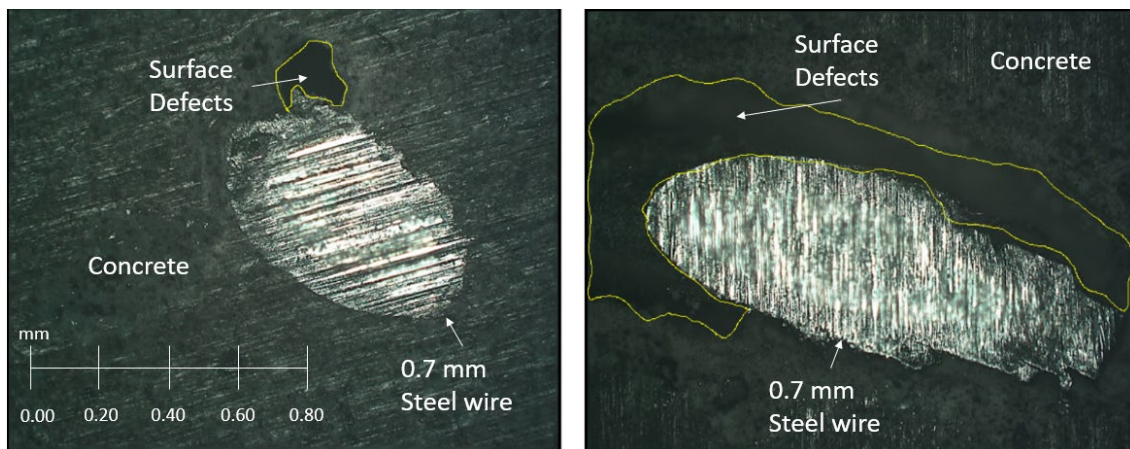


Figure 4.1 Surface Area Defects (a) 150 mm/min and (b) 200 mm/min.

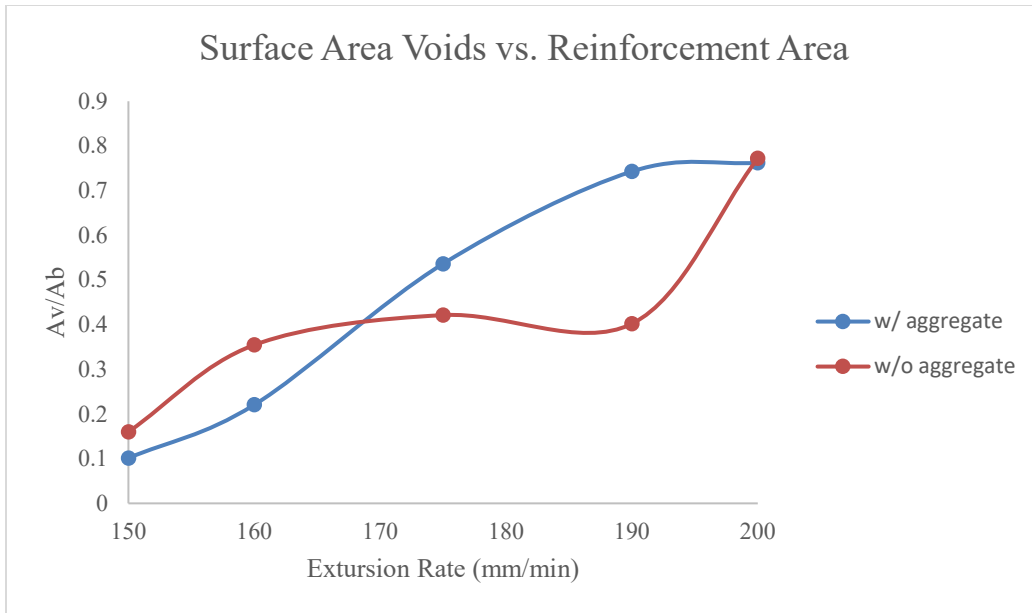


Figure 4.2 Surface Area Voids vs. Reinforcement Area.

From the optical image analysis, it was concluded that the surface defects were more likely to occur at higher extrusion rates. Figure 4.2 above illustrates the ratio of surface area defects to reinforcement surface area. As the extrusion rate increases, the quality of the samples decreases. Due to the reinforcement's rotation during printing the concrete was pushed away from the reinforcement once it was extruded out of the nozzle head. The varying velocities produced a stronger dispersion force, likely resulting in improper bonding. To prevent this, the reinforcement should be shaped prior to entering the dual-nozzle entrance. Further research will be required to reduce the potential of surface bond defects surrounding the interface of the printed specimens. Optimization between gantry, concrete, and reinforcement speeds will further need to be investigated as well. Additional samples and reinforcement printing configurations should also be investigated in future research to observe the impacts of geometrically varied

reinforcement on printed specimens. Furthermore, research will need to be conducted to analyze the volumetric defects within the samples.

#### 4.2 Results (Phase III)

As stated previously, the current system does not contain any sensing or monitoring technology. All the inputs had to be controlled manually using different program interfaces. Therefore, it was requested that controlled testing with varying parameters be used to simulate the 3D printing observations. The fresh pullout test served as a preconditioning phase of the final, cured pullout and therefore does not need to be analyzed in detail. This is because, in the fresh state, the initial yield stress of the concrete is a function of time and the material composition/preparation. “Disturbance length” and loading rate will not impact the material’s yield properties in the fresh state. The goal was to see if the initial interface bonds would be broken significantly enough to impact the cured bonding capacity.

The results of the fresh bond pullout test by settling time variation produced a trend between the concrete’s yield stress and strain. Figure 4.3 below depicts the results of the Fresh Pullout Test by Setting Time Variation. As anticipated, as the settling time increased, the resulting yield stress increased while the yield strain decreased. This indicates the progression of the concrete shifting from a fluid-like state to a solid state. In 3D printing, this can greatly impact the overall initial performance particularly with embedded reinforcement. If the reinforcement is embedded too early, there is the potential that the concrete will not be able to support the self-weight of the reinforcement. However, this parameter can be remedied with the appropriate design mix. A design mix using a lower w/c ratio will have a greater initial yield stress.

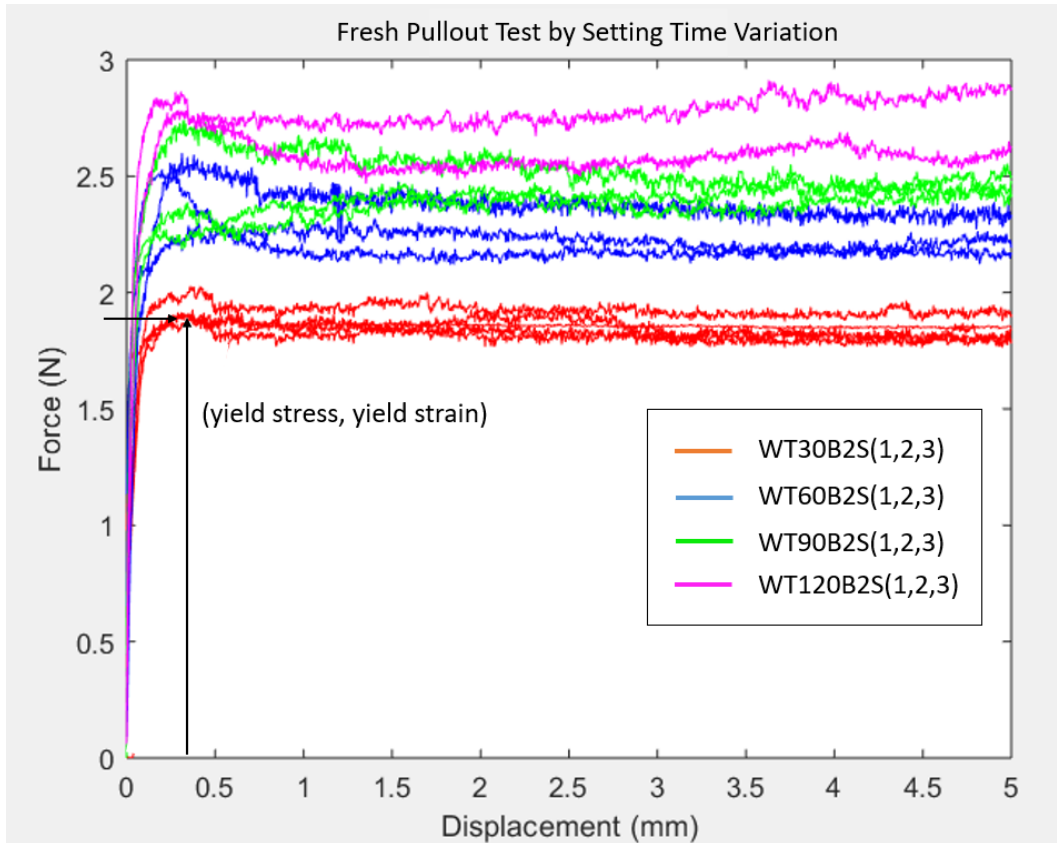


Figure 4.3 Fresh Pullout by Setting Time Variation.

Table 4.1 below depicts the averaged results gathered from Figure 4.3. As seen below, the overall yield stress of the material increases as a function of time. Inversely, the yield strain decreases as a function of time. This data indicates that the allowable “disturbance” within fresh concrete decreases as the fluidity of the concrete begins to set. Further testing in the future will need to be conducted to determine if this factor has an impact on the final bond capacity.

Table 4.1 Fresh Pullout by Setting Time Variation Test Results.

Specimen ID	Setting Time (min)	Peak Stress ( $10^2$ N/mm <sup>2</sup> )	Yield Stress ( $10^2$ N/mm <sup>2</sup> )	Yield Strain (mm/min)
WT30B2S(1,2,3)	30	2.81	2.61	0.0012
WT60B2S(1,2,3)	60	3.5	3.15	0.007
WT90B2S(1,2,3)	90	3.56	3.51	0.006
WT120B2S(1,2,3)	120	3.93	3.92	0.004

It was found that the results of the Cured Specimens Rebar Pullout Test were inconclusive. Due to irregularities in sample preparation, the resulting data was inconsistent between batch productions. 24 specimens were prepared in two batches in one session and 6 specimens were prepared in another batch in a different session. As seen below in Figure 4.4, there was a substantial difference in the final quality of the produced between mixing days. The discoloration and significant number of voids within the specimens produced on 3/21/19 produced specimens that did not perform as well as the specimens that were prepared on 4/17/19.



Figure 4.4 Inconsistent Batch Preparations.

While it is unknown whether the poor consolidation impacted the pullout strength, it can be inferred that the first mixing day's batch was not prepared correctly based on the resulting data. As seen below, the resulting force-displacement curves exhibited substantial variation in the strength capacities despite the design mix being the same for all specimens. The inconsistent batch preparation is further amplified by the fact that the resulting peak load capacity was roughly three times larger on average for the remaining 6 specimens as opposed to the original 24. This indicates that there was an error in the concrete preparation phase of the first batch of specimens.

In theory the exact same mix design was prepared in both situations. Accounting for potential discrepancies and margins of error does not explain the significant variation in the samples' strengths and therefore it can only be concluded that the original batch was prepared incorrectly. It is apparent that proper quality control of the first pour was not maintained like it was in the second pour. Furthermore, there was a significant amount of scatter amongst the remaining data which varied wildly between sample groups. There was not a clear trend that resulted from the given parameters. Of the potentially valid specimens, there are too few to draw any significant findings from. Additional samples with more adequate quality control will need to be performed before any conclusions can effectively be drawn from these parameters. Figure 4.4 below illustrates the discrepancy between the samples. Based on the current data from the experiments it is not possible to conclude that displacement rate or disturbance length and any significant impact on the overall printing process.

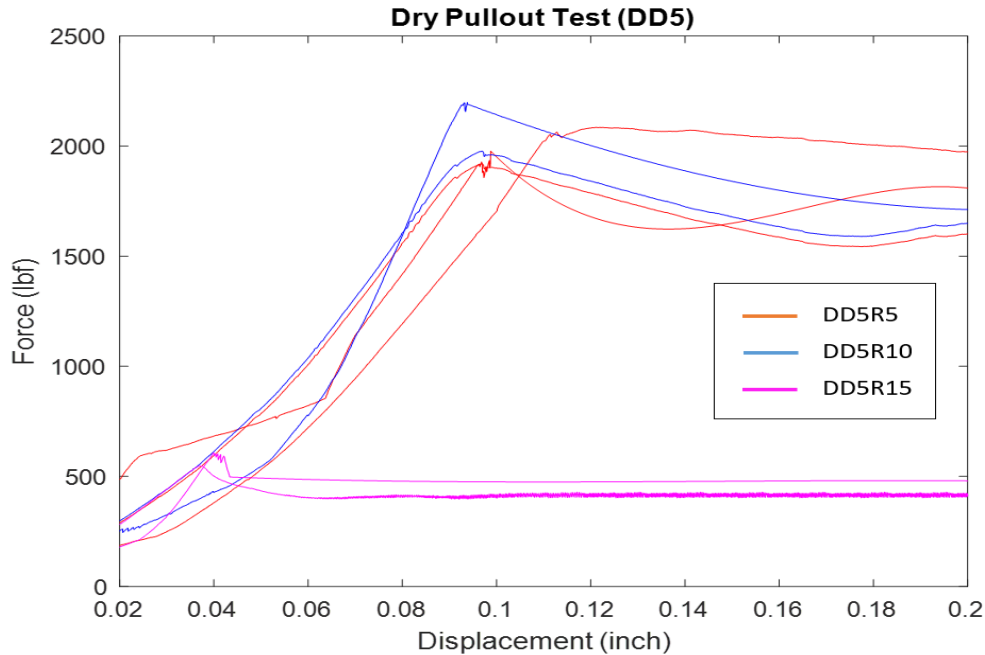


Figure 4.5 Sample Dry Pullout Test Results.

It was anticipated that specimens experiencing more disturbance at faster rates in the preconditioning phase would result in weaker overall bond capacities. This would be due to bond breakage and microcracks forming as the concrete was attempting to set. However, it should be reiterated that controlled testing does not necessarily provide an accurate substitute for printed concrete. Further experimentation will need to be conducted to correctly correlate the relationship between the disturbance length and displacement rate on final bond capacity.

Following this experiment, the remaining valid specimens (DD5R5 and DD5R10) were split open longitudinally to identify any potential defects. From the naked eye, there did not appear to be any improper bonding at the interface level like the results of the Optical Image Analysis Test from Section 3.5. Small voids did appear around the interface zone and throughout the samples cross section, however it is unlikely that these voids had any contribution regarding the dry pullout test. Further testing will need to be conducted in the future to analyze the samples

at the interface level with a microscope similar to Figures 4.1a and b. Further analysis will need to be conducted in the future to determine if the disturbance length and loading rate had an impact at the interface level.

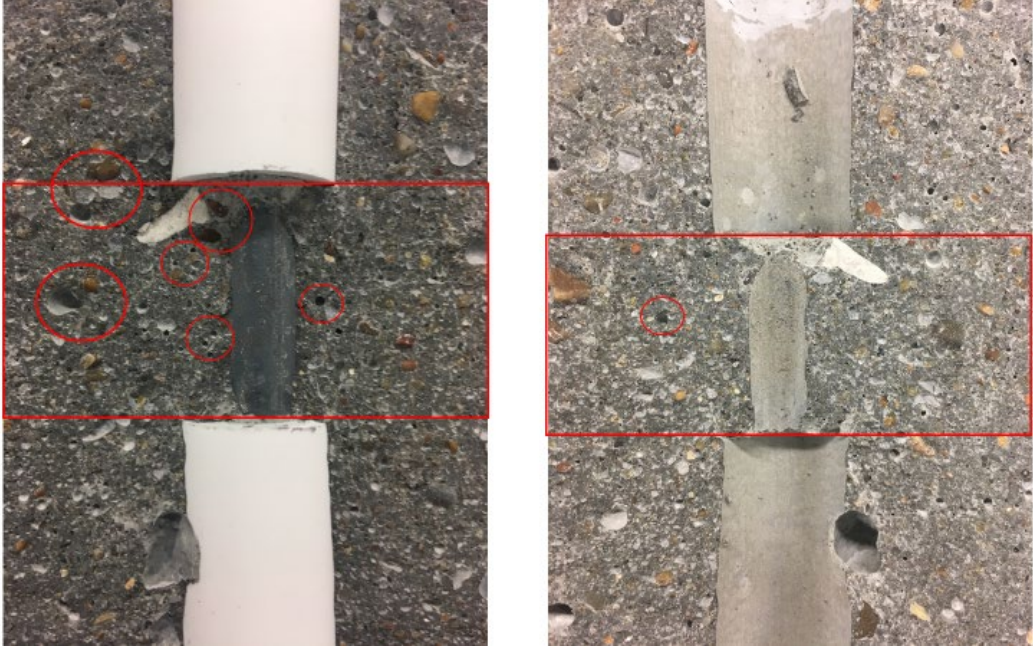


Figure 4.6 Split Concrete Test Sample.



## Chapter 5 Conclusions and Recommendations

### 5.1 Conclusions

The developments of this project came about from a consistent amount of trial and error due to the relatively new practice of 3D printing concrete with reinforcement. The overarching goal of this thesis was to provide a proof-of-concept device which could embed reinforcement into printed concrete simultaneously. Through the development phase, it was found that the introduction of actively entraining shaped reinforcement poses a significant challenge to 3D printing concrete. The concept of shaped reinforcement allows the potential for stronger anchorage, greater surface area bonding, and higher compressive strengths. However, the project's current developments only indicate the potential for this technology to be realized.

Using a reinforcement extruder as the primary embedment mechanism has its own sets of challenges and should be carefully considered. It was found that unsynchronized concrete extrusion, reinforcement extrusion, and gantry motion speeds severely damaged the quality of the printed specimens. Slower reinforcement speeds produce a dragging force which disrupts the already printed. It was also found that if the extrusion rate of the concrete and reinforcement is too high while synchronized, the reinforcement acts like that of an auger. Upon exiting the nozzle's confinement, the reinforcement pushes the concrete away disrupting the initial bond between the two materials. This was due to the reinforcement being formed from within the nozzle. When the speeds were synchronized, the quality of the prints became much more uniform. However, when observing the bond between the two interfaces at a micro level, it was found higher extrusion rates result in larger, more abundant defects between the two surfaces. As the synchronized extrusion rates increase, the more surface defects are produced.

The system at its current level is unable to effectively gauge the extrusion rates of both the concrete and reinforcement on its own (i.e. they are two separate systems). Therefore, controlled testing experiments were developed to simulate the behavior observed through the printing process. The fresh concrete preconditioning test, while technically an intermediate step for the cured pullout test, did not exhibit any significant correlation of the initial bond capacity as a function of disturbance length and displacement rate. The resulting force-displacement graph reflects this since the peak strength of fresh concrete is a function of time as well as the initial strength due to the mixed properties. The unexpected result, however, was that reaction recorded from the loading not plateau to indicate a point of yielding. This suggests that the setup was experiencing resistance due to friction despite being sealed and lubricated to prevent these build ups. This intermediate step served as a means to simulate the impacts of unsynchronized extrusion rates on the final bond capacity. Locally speaking, the displacements between the reinforcement and concrete should be zero relative to one another. This test simulates the situation where the reinforcement is extruding faster than the concrete.

Based on the results of the cured specimen's pullout test, the preconditioning test variation did not produce any significant correlation due to batch inconsistencies. Further research will be required with additional specimens. It was initially hypothesized that if both the disturbance length and displacement rate were increased in the fresh state, then the final bond capacity would decrease. The disturbance from the rebar was expected to create small micro cracks and voids along the interface between the rebar and concrete since the initial bonds were being broken locally. The interface zone surrounding the concrete and the rebar was expected to be weaker than the remaining, undisturbed zone.

The specimens in the second batch had roughly four times the capacity compared to those in the first batch. This discrepancy was on account of human error as the mix design and setup configurations were identical for both batches. Improper consolidation as well as over-lubricating the cylinder molds are the potential, observable errors. It is also possible that the material quantities were inaccurately weighed in the first batch, however this cannot be verified. As such, quality control of the first batch of specimens could not be properly maintained. Therefore, it is not acceptable to draw any significant conclusions from the data discrepancies. The lessons learned from this project will be detailed in the following section for potential improvements/alterations to the existing system and methodology.

## 5.2 Recommendations

After completion of the project, there were several design considerations and methodologies that could potentially be improved upon or incorporated in future research. It should be reiterated that the goal of this project was to contribute to a proof of concept for entraining reinforcement into printed concrete, not develop a fully functional system. As such, inefficiencies and unoptimized mechanical equipment were limiting factors in the development of this project. These limitations will be detailed in the early part of this section as a means of documenting the design flaws within this project.

The general assembly of the device will require upgrading for future research. For starters, the designed 3D printer needs a more efficient and effective extrusion system. The mortar gun is originally designed to be held manually, with the hopper positioned vertically relative to the ground. Furthermore, the extrusion speed is expected to be significantly higher than what is currently used for machine-controlled printing process. As such this affects the effectiveness of the print in two ways. First, the hopper is positioned horizontally, making it

difficult for the flow of paste/mortar to travel through the device. The mortar had to be manually pushed through the system during prints as the slow extrusion speed and high viscosity of the mortar would not allow the mortar to flow through the system on its own. Second, due to the slower extrusion rate the consolidating vibrator, located within the hopper, could not effectively assist in increasing the flow of mortar through the system. Finally, the slower rate also had an impact on the minimum aggregate size that could be extruded. During testing, a majority of the prints could only use a mixture of cement and water, as the mortar gun would effectively clog up with the addition of aggregates (>1 mm). When handheld, the device could easily extrude this material, but due to the positioning and machine printing speed, some of its functionality was reduced. The proposed solution is to design an auger with hopper that is mounted vertically for the mortar to directly flow through the system unhindered. Furthermore, increasing the auger size and motor capacities would greatly increase the amount of mortar that could be extruded consistently. The current stepper motor does not have a sufficient amount of torque to rotate the auger when the sand/binder ratio is larger than 1:2 and should be upgraded accordingly.

Concerning the reinforcement extrusion components, there are several notable inefficiencies with the current setup. For starters the material itself is fed through a small, pre-shaped mold using a stepper motor to drive the material through the system. It was found that due to the high ductility of the wire material coupled with the surface roughness of the interior tube, the material would become lodged in the tube preventing it from extruding. During the trials with successful extrusions, the exiting portion of the tube would become clogged with mortar once again preventing extrusions from occurring. This made it challenging to successfully print a sufficient and continuous reinforced member consistently. Moving forward, it is

recommended to redesign the fiber extrusion system currently selected and to focus on perfecting non-shaped reinforcement before developing a system that can print helix shaped geometry.

The final major inefficiency with the system is the movability of the printer. The motion capacity of the design is significantly limited due to the bulky nature of both the mortar gun and the fiber extrusion component. Realistically, the current setup is only capable of extruding linearly without the ability to print multiple layers easily. It is strongly recommended to convert the horizontal nozzle to a vertical nozzle to allow for greater directional printing freedom. This change will greatly impact the fiber extrusion component as well, as it is currently dependent upon the nozzle's secondary entrance point.

Despite these inherent inefficiencies and imperfections, the concept of incorporating reinforcement still exists. The new proposed solution is to focus on optimizing and accurately integrating straight reinforcement into the system before helix shaped reinforcement is printed. The solution still utilizes the original gantry and extrusion system while eliminating the necessity actively extrude/control the reinforcement. Rather than using a motor to try and synchronize the extrusions and gantry speed, the reinforcement can be anchored/tied to an external support where it is unraveled from the spool as the gantry system moves. This ensures that the correct amount of reinforcement will be "extruded" from the system and it secures the location of the reinforcement within the concrete. A major issue with the first system was that it was impossible to separate the continuous length of the reinforcement without damaging the surrounding concrete. This method will operate in three simple steps: (1) The reinforcement will be unraveled from the spool as the gantry system is moving while the concrete is being printed around it, (2) the flow of concrete will stop but the gantry will continue to move for roughly 2" inches, (3) after the system has stopped, the exposed reinforcement can be cut and separated from the

system. This is the desired method of separation because it allows the reinforcement to be printed again without having to “reload” the spool in the system. It will merely need to be dragged out again and anchored to a new position. This could even allow for layered extrusions, as the reinforcement could be anchored at different heights of the vertical anchoring support.

Conveniently, the smooth surface of the horizontal nozzles surface could act as a means of smoothing the top layer of the extruded concrete as a secondary layer is being added. The final change to make this design more effective is to reconfigure the nozzles opening diameter.

Converting from a purely circular 5cm opening to a smaller, rectangular opening with chamfered sides would allow for easier layer by layer deposition. Since the reinforcement will only be “extruded” if it is anchored, multiple layers can be printed over the initial one to provide sufficient cover. This method will ensure that appropriate bond and bending strength testing can be completed. Moving forward, it is highly recommended to take this approach when working on the new design.

Considering 3D printing reinforcement by an extrusion technique, there are several notable recommendations for future developments. A key component of printing concrete with reinforcement is the ability to synchronize the extrusion rates of both materials. Sensing technology will also need to be incorporated into the system once it has been upgraded with the above recommendations. The concept of using controlled experiments to represent the 3D printing process cannot effectively be relied upon due to the reliance on the concrete behaving as if it is being extruded. Due to the complex nature of the interacting mechanisms between the flow of concrete and reinforcement, it is currently too difficult to effectively quantify and extrapolate data from the current system.

## References

- [1] Buswell R., Silva W., Jones S., & Dirrenberger. (2018). 3D Printing Using Concrete Extrusion: A Roadmap for Research. *Cement and Concrete Research*, 112, 37-49.
- [2] Camacho D., Clayton P., O'Brien W., Ferron R., et. all. (2017) Applications of Additive Manufacturing in the Construction Industry – A Prospective Review. 34<sup>th</sup> International Symposium on Automation and Robotics in Construction
- [3] Wangler T., Lloret E., Reiter L., Hack N., Gramazio F., et. all. (2016). Digital Concrete: Opportunities and Challenges. *RILEM Technical Letters*, 67-75.
- [4] Yossef M. & Chen A. (2015) Applicability and Limitations of 3D Printing for Civil Structures. *Civil, Construction and Environmental Engineering Conference Presentations and Proceedings*. 35.
- [5] Khoshnevis, R. Dutton, Innovative Rapid Prototyping Process Makes Large Sized, Smooth Surfaced Complex Shapes in a Wide Variety of Materials, *Mater. Technol.* 13 (1998) 53–56.
- [6] Khoshnevis, B., Hwang, D., Yao, K., & Yeh, Z. (2006). Mega-scale fabrication by contour crafting. *Int. J. Industrial and Systems Engineering*, 1(3), 301-320.
- [7] <http://www.winsun3d.com> (April 14, 2019).
- [8] [totalkustom.com](http://totalkustom.com). 3D Concrete House Printer (March 23, 2019).
- [9] Wolfs R. (2015). 3D Printing of Concrete Structures. Eindhoven University of Technology.
- [10] Shakor P., Renneberg J., Nejadi S., and Paul G. (2017). Optimisation of Different Concrete Mix Designs for 3D Printing by Utilising 6DOF Industrial Robot. 34th International Symposium on Automation and Robotics in Construction.
- [11] <https://cybe.eu/3d-concrete-printers>. CyBe Construction, (April 14, 2019)
- [12] Anderson, S. (2015). Concrete Plans: CyBe's Berry Hendriks Describes Plans to 3D Print with Mortar.
- [13] <https://www.aniwaa.com/house-3d-printer-construction/>. Aniwaa, (March 3, 2019).
- [14] [contourcrafting.com](http://contourcrafting.com). Contour Crafting Corporation, 2017 (March 3, 2019).
- [15] Asprone D., Auricchio F., Menna C., & Mercuri V. (2018). 3D Printing of Reinforced Concrete Elements: Technology and Design Approach. *Construction and Building Materials*, 165, 218-231.

- [16] Asprone D., Menna C., Bos F., Salet T., Mata-Falcon J., & Kaufmann W. (2018). Rethinking Reinforcement for Digital Fabrication with Concrete. *Cement and Concrete Research*.
- [17] Bos. F., Ahmed Z., Jutinov E., & Salet. T. (2017) Experimental Exploration of Metal Cable as Reinforcement in 3D Printed Concrete. *Materials*, 10.
- [18] Lim, S., Buswell, R., Le, T., Austin, S., Gibb, A., & Thorpe, T. (2012). Developments in construction-scale additive manufacturing processes. *Automation in Construction*, 21, 262-268.
- [19] Malaeb Z., Hachem H., Tourbah A., Mallouf T., Zarwi N., & Hamzeh F. (2015). 3D Concrete Printing: Machine and Mix Design. *IJCIET*, 14-22.
- [20] Jeong H., Han, S., Choi S., Lee Y., Yi S., and Kim K. (2019). Rheological property Criteria for Buildable 3D Printing Concrete. *Materials*, 12.
- [21] Lediag R., and Kruger, D. (2017). Optimizing concrete mix design for application in 3D printing technology for the construction industry. *Solid State Phenomena*.
- [22] Oxman, N., Keating, S., & Tsai, E. (2011). Functionally Graded Rapid Prototyping Innovative Developments in Virtual and Physical Prototyping'. *Proceedings of the 5th International Conference on Advanced Research in Virtual and Rapid Prototyping*.
- [23] Bos F., Wolfs R., Ahmed Z. & Salet T. (2016) Additive manufacturing of concrete in construction: potentials and challenges of 3D concrete printing. *Virtual and Physical Prototyping*, 209-22
- [24] Le, T., Austin, S., Lim, S., Buswell, R., Law, R., Gibb, A., et al. (2012). Hardened properties of high-performance printing concrete. *Cement and Concrete Research*, 42, 558-566.
- [25] Le, T., Austin, S., Lim, S., Buswell, R., Law, R., Gibb, A., et al. (2011). Mix design and fresh properties for high-performance printing concrete. *Materials and Structures*, 1221-1232.